4560 *Inorg. Chem.* **2010**, *49*, 4560–4569
DOI: 10.1021/ic1001013

Inorganic Chemistry
Article

Doubly Pyrazolate-Bridged Dinuclear Complexes of a Highly Constrained Bis-terdentate Ligand: Observation of a [High Spin-Low Spin] State for $[Fe^{II}_2(PMAP)_2][SbF_6]_2 \cdot 2.25(C_3H_8O)$ (PMAP = 3,5-bis{[*N*-(2-pyridylmethyl)amino]-methyl}-1*H*-pyrazolate)

Andy Noble,[†,∥] Juan Olguín,[†] Rodolphe Clérac,[‡,§] and Sally Brooker*[,†]

[†]*Department of Chemistry and The MacDiarmid Institute for Advanced Materials and Nanotechnology, University of Otago, PO Box 56, Dunedin, New Zealand,* [‡]*CNRS, UPR 8641, Centre de Recherche Paul Pascal (CRPP), Equipe "Matériaux Moléculaires Magnétiques", 115 avenue du Dr. Albert Schweitzer, Pessac, F-33600, France, and* [§]*Université de Bordeaux, UPR 8641, Pessac, F-33600, France.* [∥] *Present address: Stratingh Institute for Chemistry, University of Groningen, Nijenborgh 4, 9747 AG Groningen, The Netherlands.*

Received January 17, 2010

The bis-terdentate pyrazole-based ligand 3,5-bis{[*N*-(2-pyridylmethyl)amino]methyl}-1*H*-pyrazole (PMAPH) was synthesized from 3,5-(1*H*)-pyrazoledicarbaldehyde and 2 equiv of 2-(aminomethyl)pyridine, using sodium borohydride to reduce the imine intermediate. A family of dinuclear complexes $[M^{II/III}_2(PMAP)_2](X)_{2/4}$ was prepared by 2:2:2 reactions of MX_2/PMAPH/base, where M = Zn^{II} and X = BF_4^-; M = Cu^{II} and X = ClO_4^-, BF_4^-, OAc^-, NO_3^-; M = Ni^{II}, Fe^{III} and X = ClO_4^-, BF_4^-; M = Fe^{II} and X = SbF_6^-. Single crystal X-ray structure determinations on four complexes: $[Fe^{III}_2(PMAP)_2](BF_4)_4 \cdot 2MeCN$, $[Ni^{II}_2(PMAP)_2](ClO_4)_2 \cdot 2MeCN$, $[Cu^{II}_2(PMAP)_2](BF_4)_2 \cdot 2MeCN$, and $[Zn^{II}_2(PMAP)_2](BF_4)_2 \cdot 2MeCN$ confirmed a dinuclear doubly pyrazolate-bridged structure for each. The two metal centers in these complexes have similar N_6 distorted octahedral coordination spheres, with all donors provided by the two deprotonated $PMAP^-$ ligands. Magnetic measurements reveal intra-dinuclear antiferromagnetic interactions for both the M = Cu^{II} and Ni^{II} $[M_2(PMAP)_2](BF_4)_4$ complexes, with $J/k_B = -252(2)$ K and $J/k_B = -24.7(2)$ K ($H = -2JS_MS_M$), respectively. Interestingly magnetic measurements show that the complex $[Fe^{II}_2(PMAP)_2](SbF_6)_2 \cdot 2.25(C_3H_8O)$ is in a mixed high spin (HS)-low spin (LS) spin state, [HS-LS], from 300 to 1.8 K, with no sign of spin crossover to a fully low spin form [LS-LS] even at 1.8 K.

Introduction

The dicarbonyl heterocycles 3,6-diformylpyridazine,[1] 3,5-acetyl-1,2,4-triazolate,[2,3] 3,5-dibenzoyl-1,2,4-triazolate,[2] and 3,5-diformylpyrazole[4−6] (Figure 1) are useful starting materials for creating more complex and interesting compounds. Some of the resulting complexes have shown intriguing properties, usually because pyrazoles, triazoles, and pyridazines all have adjacent nitrogen atoms capable of bridging two distinct metal centers upon complexation thus facilitating potentially intriguing chemical reactivity,[6−8] and electrochemical[9] and magnetic[10,11]

*To whom correspondence should be addressed. E-mail: sbrooker@chemistry.otago.ac. Phone: +64 3 479 7919. Fax: +64 3 479 7906.

(1) Brooker, S.; Kelly, R. J. *J. Chem. Soc., Dalton Trans.* **1996**, 2117–2122. Wiley, R. H. *J. Macromol. Sci., Chem.* **1987**, *24*(10), 1183–1190.
(2) Brandt, C. D.; Kitchen, J. A.; Beckmann, U.; White, N. G.; Jameson, G. B.; Brooker, S. *Supramol. Chem.* **2007**, *19*, 17–27.
(3) de Mendoza, J.; Ontoria, J. M.; Ortega, M. C.; Torres, T. *Synthesis* **1992**, 398–402.
(4) de Geest, D. J.; Noble, A.; Moubaraki, B.; Murray, K. S.; Larsen, D. S.; Brooker, S. *Dalton Trans.* **2007**, 467–475.
(5) Kumar, M.; Arán, V. J.; Navarro, P. *Tetrahedron Lett.* **1995**, *36*(12), 2161–2164.
(6) Noël, G.; Röder, J. C.; Dechert, S.; Pritzkow, H.; Bolk, L.; Mecking, S.; Meyer, F. *Adv. Synth. Catal.* **2006**, *348*(7−8), 887–897.
(7) Beckmann, U.; Ewing, J. D.; Brooker, S. *Chem. Commun.* **2003**, 1690–1691.
(8) Itoh, M.; Motoda, K.; Shindon, K.; Kamiusuki, T.; Sakiyama, H.; Matsumoto, N.; Okawa, H. *J. Chem. Soc., Dalton Trans.* **1995**, 3635–3641.
(9) Lan, Y.; Kennepohl, D. K.; Moubaraki, B.; Murray, K. S.; Cashion, J. D.; Jameson, G. B.; Brooker, S. *Chem.—Eur. J.* **2003**, *9*, 3772–3784 and front cover feature. Brooker, S.; Ewing, J. D.; Ronson, T. K.; Harding, C. J.; Nelson, J.; Speed, D. J. *Inorg. Chem.* **2003**, *42*, 2764–2773. Brooker, S.; Davidson, T. C.; Hay, S. J.; Kelly, R. J.; Kennepohl, D. K.; Plieger, P. G.; Moubaraki, B.; Murray, K. S.; Bill, E.; Bothe, E. *Coord. Chem. Rev.* **2001**, *216−217*, 3–30. Brooker, S.; Hay, S. J.; Plieger, P. G. *Angew. Chem., Int. Ed.* **2000**, *39*, 1968–1970. Brooker, S.; Kelly, R. J.; Plieger, P. G. *Chem. Commun.* **1998**, 1079–1080. Brooker, S.; Kelly, R. J.; Moubaraki, B.; Murray, K. S. *Chem. Commun.* **1996**, 2579–2580.
(10) Klingele, M. H.; Moubaraki, B.; Cashion, J. D.; Murray, K. S.; Brooker, S. *Chem. Commun.* **2005**, 987–989. Grunert, C. M.; Reiman, S.; Spiering, H.; Kitchen, J. A.; Brooker, S.; Gütlich, P. *Angew. Chem., Int. Ed.* **2008**, *47*, 2997–2999.
(11) Brooker, S.; de Geest, D. J.; Kelly, R. J.; Plieger, P. G.; Moubaraki, B.; Murray, K. S.; Jameson, G. B. *J. Chem. Soc., Dalton Trans.* **2002**, 2080–2087. Brooker, S.; Plieger, P. G.; Moubaraki, B.; Murray, K. S. *Angew. Chem., Int. Ed.* **1999**, *38*, 408–410 and front cover feature.

 Published on Web 04/15/2010

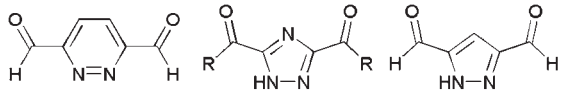

Figure 1. Selection of dicarbonyl head units used by our research group, and others, to form macrocycles and acyclic ligands (R = CH_3 or C_6H_5).

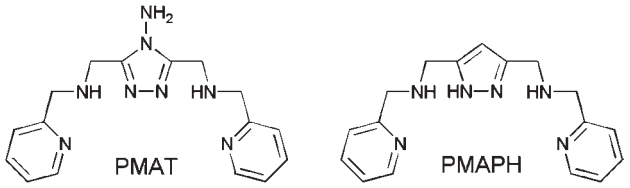

Figure 2. Structure of the ligands PMAT[16] and PMAPH.

properties. These moieties have also been shown to possess the appropriate field strength to allow for spin crossover (SCO) with the metal ions iron(II)[12] and cobalt(II).[13] There is currently great interest in SCO phenomena of iron(II), iron(III), cobalt(II), and manganese(III) ions.

SCO active pyrazolate complexes of iron(II) have been synthesized by the groups of Murray[14] and Kaizaki,[15] and it is this potential we wish to explore by using pyrazole analogues, such as PMAPH, of our previously investigated bis-terdentate 1,2,4- triazole ligand[16] systems, such as PMAT (Figure 2, and see later). The iron(II) complex of PMAT, $[Fe^{II}_2(PMAT)_2](BF_4)_2 \cdot DMF$, exhibits SCO from fully high spin (HS) form [HS-HS] to mixed high spin (HS)-low spin (LS) spin state [HS-LS] at about 225 K and provided the first example of a structurally characterized [HS-LS] complex.[10,17]

Triazole, pyrazole, and pyridazine moieties are also known to mediate spin exchange between N^1N^2-bridged metal ions. The ability to link metal centers together to create a two, or possibly three, way switch, with communication between metal centers, opens the door to fascinating and potentially very useful compounds in the area of nanotechnology, specifically the development of nanoswitches.[18] Such complexes are also of interest in the area of biomimics (vide infra).[8,19]

A number of different research groups have synthesized and investigated polydentate ligands which provide a bridging pyrazolate, similar to PMAPH. Indeed, Okawa and co-workers

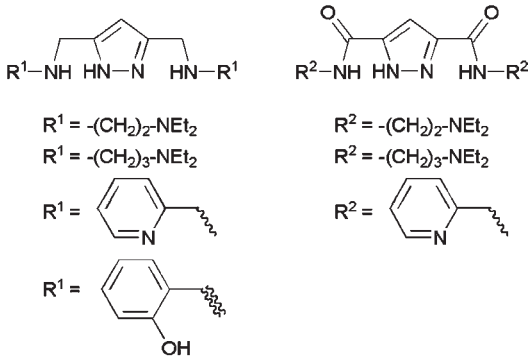

Figure 3. Selection of the bis-terdentate pyrazole ligands prepared by Okawa and co-workers.[8,20–22] PMAPH is LHS with R^1 = 2-pyridyl; $PMDPH_3$ is RHS with R^1 = 2-pyridyl.

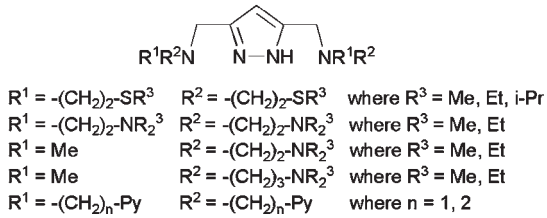

Figure 4. Selection of bis-terdentate and bis-tetradentate pyrazole ligands prepared by Meyer and co-workers.[19,23,24]

have previously prepared the ligand PMAPH, albeit by a different synthetic route (Scheme 1). They have also prepared a number of similar acyclic ligands (Figure 3) which were used to complex mainly manganese(II),[8] manganese(III),[20] and copper(II).[21] All of these ligands are bis-terdentate and provide a central pyrazole moiety which is deprotonated and bridges the two metal centers in the resulting complexes. The $[Mn^{II}_2(PMAP)_2](BPh_4)_2$ complex,[8] prepared using sodium methoxide as a base, displayed catalase-like activity: it was found to increase the rate of disproportionation of hydrogen peroxide.

Meyer and co-workers have also prepared a wide range of acyclic bis-terdentate and bis-tetradentate pyrazole ligands (Figure 4). Their work in this area has contributed strongly to a number of topics, including zinc(II) complexes[19] as biomimics for phosphatases and lactamases, and nickel(II) azido bridged complexes.[23] Most recently they have ventured into the area of [2 × 2] grid-like complexes, specifically of copper-(II) and nickel(II) with the pyrazole diamide $PMDPH_3$ ligand[24] (which had been reported earlier by Okawa, Figure 3,[22]). As we reported previously, for [2 × 2] grid complexes of pyrazine diamide ligands, they too exploit the

(12) van Koningsbruggen, P. J. *Top. Curr. Chem.* **2004**, *233*, 123–149.
(13) Goodwin, H. A. *Top. Curr. Chem.* **2004**, *234*, 23–47.
(14) Schneider, C. J.; Cashion, J. D.; Moubaraki, B.; Neville, S. M.; Batten, S. R.; Turner, D. R.; Murray, K. S. *Polyhedron* **2007**, *26*, 1764–1772. Leita, B. A.; Moubaraki, B.; Murray, K. S.; Smith, J. P. *Polyhedron* **2005**, *24*, 2165–2172. Leita, B. A.; Moubaraki, B.; Murray, K. S.; Smith, J. P.; Cashion, J. D. *Chem. Commun.* **2004**, 156–157.
(15) Kaizaki, S.; Nakano, K.; Suemura, N.; Yoneda, K.; Kawata, S. *Dalton Trans.* **2005**, 740–743. Nakano, K.; Suemura, N.; Kawata, S.; Fuyuhiro, A.; Yagi, T.; Nasu, S.; Morimoto, S.; Kaizaki, S. *Dalton Trans.* **2004**, 982–988. Nakano, K.; Kawata, S.; Yoneda, K.; Fuyuhiro, A.; Yagi, T.; Nasu, S.; Morimoto, S.; Kaizaki, S. *Chem. Commun.* **2004**, 2892–2893.
(16) Klingele, M. H.; Moubaraki, B.; Murray, K. S.; Brooker, S. *Chem.—Eur. J.* **2005**, *11*, 6962–6973.
(17) Bhattacharjee, A.; Ksenofontov, V.; Kitchen, J. A.; White, N. G.; Brooker, S.; Gütlich, P. *Appl. Phys. Lett.* **2008**, *92*, 174104.
(18) Letard, J.-F.; Guionneau, P.; Capes, L. *Top. Curr. Chem.* **2004**, *235*, 221–249.
(19) Bauer-Siebenlist, B.; Dechert, S.; Meyer, F.; Farkas, E.; Vidovic, D. *Chem.—Eur. J.* **2005**, *11*, 4349–4360. Bauer-Siebenlist, B.; Dechert, S.; Meyer, F. *Chem.—Eur. J.* **2005**, *11*, 5343–5352. Meyer, F.; Pritzkow, H. *Eur. J. Inorg. Chem.* **2005**, 2346–2351. Bauer-Siebenlist, B.; Meyer, F.; Farkas, E.; Vidovic, D.; Cuesta-Seijo, J. A.; Herbst-Irmer, R.; Pritzkow, H. *Inorg. Chem.* **2004**, *43*(14), 4189–4202. Bauer-Siebenlist, B.; Meyer, F.; Vidovic, D.; Pritzkow, H. *Z. Anorg. Allg. Chem.* **2003**, *629*, 2152–2156.
(20) Okawa, H.; Shindo, K.; Mori, Y.; Motoda, K.; Sakiyama, H.; Matsumoto, N. *Inorg. Chem.* **1992**, *31*, 4987–4990.
(21) Kamiusuki, T.; Okawa, H.; Matsumoto, N.; Kida, S. *J. Chem. Soc., Dalton Trans.* **1990**, 195–198.
(22) Kamiusuki, T.; Okawa, H.; Kitaura, E.; Koikawa, M.; Matsumoto, N.; Kida, S. *J. Chem. Soc., Dalton Trans.* **1989**, 2077–2081.
(23) Demeshko, S.; Leibeling, G.; Dechert, S.; Meyer, F. *Dalton Trans.* **2006**, 3458–3465. Demeshko, S.; Leibeling, G.; Maringgele, W.; Meyer, F.; Mennerich, C.; Klauss, H.-H.; Pritzkow, H. *Inorg. Chem. Commun.* **2005**, *44*(3), 519–528. Leibeling, G.; Demeshko, S.; Dechert, S.; Meyer, F. *Angew. Chem., Int. Ed.* **2005**, *44*, 7111–7114. Leibeling, G.; Demeshko, S.; Bauer-Siebenlist, B.; Meyer, F.; Pritzkow, H. *Eur. J. Inorg. Chem.* **2004**, 2413–2420. Meyer, F.; Kircher, P.; Pritzkow, H. *Chem. Commun.* **2003**, 774–775.
(24) Klingele (née Hausmann), J.; Prikhodko, A. I.; Leibeling, G.; Demeshko, S.; Dechert, S.; Meyer, F. *Dalton Trans.* **2007**, *20*, 2003–2013.

Scheme 1. Two Synthetic Methods That Have Been Employed for the Synthesis of the Ligand PMAPH[a] and Then of the Transition Metal Complexes[b]

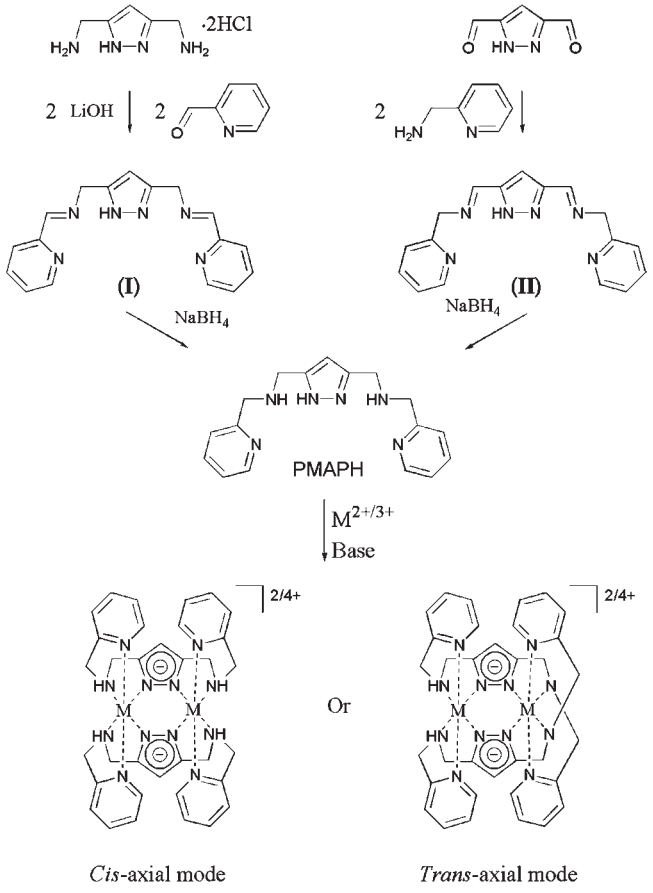

[a] LHS Owaka and co-workers,[8] RHS this paper.

[b] The *cis*-axial and *trans*-axial coordination modes of $PMAP^-$ observed (vide infra) are shown.

deprotonation of the amide and the rigidity of the diamidoheterocyclic ligand to facilitate access to grids.[25]

In this paper we report the synthesis and characterization of the pyrazole containing bis-terdentate ligand, PMAPH, from 3,5-(1*H*)-pyrazoledicarbaldehyde and 2 equiv of 2-(aminomethyl)pyridine followed by reduction, and a family of first row transition metal complexes of that ligand. Also reported are the X-ray crystal structures of four complexes: $[M^{II}_2(PMAP)_2](BF_4)_2 \cdot S$ where M = Zn and Cu, $[Fe^{III}_2(PMAP)_2](BF_4)_4 \cdot 2MeCN$, and $[Ni^{II}_2(PMAP)_2](ClO_4)_2 \cdot 2MeCN$.

Results and Discussion

Synthesis of PMAPH ligand. A synthesis of the ligand PMAPH, using an alternative route to the one presented here, has previously been described by the group of Okawa[8] (Scheme 1). They made use of 3,5-di(aminomethyl)pyrazole dihydrochloride, prepared by them previously,[26] which was first neutralized by lithium hydroxide, then reacted with commercially available 2-pyridine-2-carbaldehyde to form an imine, (**I**). In the final step of this one pot reaction (**I**) was reduced by sodium borohydride to give the ligand, PMAPH, as a yellow oil. No overall yield was reported. Here we report the synthesis of the same ligand by an alternative method using 3,5-(1*H*)-pyrazoledicarbaldehyde, which was synthesized by the methods described by Vogel[27c], Bosnich et al.[27b], and Navarro et al.[27a] and their co-workers.[27] The 3,5-(1*H*)-pyrazoledicarbaldehyde was added to 2 equiv of 2-(aminomethyl)pyridine in methanol. This generates imine (**II**), an analogue of (**I**), which is also reduced in situ using sodium borohydride (Scheme 1). The overall yield of PMAPH, obtained as a light yellow oil, from 3,5-(1*H*)-pyrazoledicarbaldehye via (**II**), was 85%. The oil was found to be of sufficient purity, by ^1H NMR analysis, to be used in subsequent reactions without any further purification.

Synthesis of Complexes of PMAPH. The ligand PMAPH is expected to deprotonate and act as a bis-terdentate monoanionic ligand. When a 2:2 ratio of $M^{x+}/PMAP^-$ is employed this should result in $[M_2(PMAP)_2]^{(2x-2)+}$ complexes in which two metal centers are "sandwiched" by two bis-terdentate ligands, resulting in two six coordinate metal ions (Scheme 1). As stated earlier, this type of compound has more than a passing resemblance to the triazole-based complex $[Fe^{II}_2(PMAT)_2](BF_4)_4 \cdot DMF$, which had exhibited unique SCO behavior.[10] Pyrazolate-based ligands have also been used, most notably by Murray[14] and Kaizaki,[15] to prepare, usually under inert gas protection, SCO-active compounds of iron(II). Currently the only reported complex of the PMAPH ligand is the dinuclear complex $[Mn^{II}_2(PMAP)_2](BPh_4)_2$ described by Okawa and co-workers.[8] We were therefore interested in complexing PMAPH with transition metal ions other than manganese(II), most especially with iron(II). Because of difficulties in the synthesis of iron(II) complexes (see below), we decided to analyze the reactivity of PMAPH ligand by synthesizing other first row transition metal complexes [copper(II), nickel(II), and zinc(II)] to try to understand its chemistry.

The reaction of PMAPH with $Ni(ClO_4)_2 \cdot 6H_2O$ in a 2:2 ratio in acetonitrile at room temperature initially gave a pink powder, and subsequently pink crystals by diethyl ether vapor diffusion, in a combined yield of 50%. Elemental analysis of the powder was consistent with the formula $[Ni^{II}_2(PMAP)_2](ClO_4)_2 \cdot MeCN$. The pink single crystals, $[Ni^{II}_2(PMAP)_2](ClO_4)_2 \cdot 2MeCN$, were suitable for single crystal structure analysis (vide infra). The infrared spectrum displayed peaks consistent with the presence of perchlorate counteranions, at 1086 and 626 cm^{-1}.

The complex $[Ni^{II}_2(PMAP)_2](BF_4)_2 \cdot 1.5H_2O$ was synthesized in a similar manner as the perchlorate analogue but using 2 equiv of $Ni(BF_4)_2 \cdot 6H_2O$, PMAPH, and triethylamine in acetonitrile at room temperature. A second

(25) Klingele (née Hausmann), J.; Boas, J. F.; Pilbrow, J. R.; Moubaraki, B.; Murray, K. S.; Berry, K. J.; Hunter, K. A.; Jameson, G. B.; Boyd, P. D. W.; Brooker, S. *Dalton Trans.* **2007**, 633–645 and front cover image. Klingele-(née Hausmann), J.; Moubaraki, B.; Murray, K. S.; Boas, J. F.; Brooker, S. *Eur. J. Inorg. Chem.* **2005**, 1530–1541. Hausmann, J.; Brooker, S. *Chem. Commun.* **2004**, 1530–1531. Hausmann, J.; Jameson, G. B.; Brooker, S. *Chem. Commun.* **2003**, 2992–2993.

(26) Kamiusuki, T.; Okawa, H.; Inoue, K.; Matsumoto, N.; Kodera, M.; Kida, S. *J. Coord. Chem.* **1991**, *23*, 201–211. Kamiusuki, T.; Okawa, H.; Kitaura, E.; Koikawa, M.; Matsumoto, N.; Kida, S.; Oshio, H. *J. Chem. Soc., Dalton Trans.* **1989**, 2077–2081.

(27) (a) Kumar, M.; Arán, V. J.; Navarro, P. *Tetrahedron Lett.* **1993**, *34* (19), 3159–3162. (b) Schenck, T. G.; Downes, J. M.; Milne, C. R. C.; MacKenzie, P. B.; Boucher, H.; Whelan, J.; Bosnich, B. *Inorg. Chem.* **1985**, *24*, 2334–2337. (c) Vogel, A. I., *Vogel's Textbook of Practical Organic Chemistry*, 4th ed.; Wiley, John & Sons, Incorporated: London, 1978; p 881.

recrystallization by diethyl ether vapor diffusion into the pink solution afforded pink crystals with elemental analysis data consistent with the formula $[Ni^{II}_2(PMAP)_2](BF_4)_2 \cdot 1.5H_2O$. The IR spectrum shows the characteristic bands for BF_4^- at 1083, 1051, and 628 cm^{-1}.

The 2:2 reactions of PMAPH with copper(II) tetrafluoroborate, perchlorate, nitrate, or acetate, in the presence of a stoichiometric amount of base except for the acetate salt, in all cases gave blue solids, $[Cu^{II}_2(PMAP)_2]X_2 \cdot$ solvent, in yields of 32 to 63%. Single crystals of the X = BF_4^- complex were grown and analyzed by X-ray diffraction (vide infra).

Use of copper(II) acetate, as the acetate ions are slightly basic, meant that an additional base was not necessary for the deprotonation of the PMAPH. Interestingly, each of the other dicopper(II) complexes can also be synthesized without a base as copper(II) is known to compete quite well with H^+ for amide nitrogen atoms.[28] However, the yields are found to be lower in the absence of a base.

As expected, all of these copper(II) complexes had very similar infrared spectra indicating that the core, $[Cu^{II}_2(PMAP)_2]^{2+}$, was present in all cases. Only the anions created significant differences: BF_4^- peaks at 1084 and 624 cm^{-1}, ClO_4^- peaks at 1087 and 624 cm^{-1}, NO_3^- peak at 1354 cm^{-1}, and OAc^- with the asymmetric and symmetric stretches at 1568 and 1404 cm^{-1}, respectively. The difference between the two acetate peaks, 164 cm^{-1}, is indicative of an ionic carboxylate group.[29] This implies that this potentially coordinating anion does not displace the pyrazole-based ligands, but rather that the central core, $[Cu^{II}_2(PMAP)_2]^{2+}$, is favored over species involving coordinated counteranions. However, this was not tested further, for example, by trying a more strongly coordinating anion or by employing a 2:1 metal to ligand ratio, as this was not of key interest to us in this study.

The 2:2:2 reaction ratio of zinc(II) tetrafluoroborate, PMAPH, and base was used to synthesize the $[Zn^{II}_2(PMAP)_2](BF_4)_2 \cdot H_2O$ complex. Unlike in the previous reactions, as zinc(II) tends to be slightly acidic, a base was required to obtain a clean sample of the desired complex. Initially triethylamine was used; however, after vapor diffusion of diethyl ether into the reaction solution, a sticky tar-like product was obtained. When potassium *tert*-butoxide was used instead, the dinuclear zinc(II) complex was obtained as a crystalline material, with crystals that were suitable for X-ray crystallography (vide infra), in 52% yield. The IR spectrum had BF_4^- peaks at 1052 and 624 cm^{-1}.

In contrast to the relatively straightforward reactions of PMAPH with zinc(II), copper(II), and nickel(II), the analogous Fe^{II} chemistry was far more challenging (see Supporting Information for a detailed discussion). This was not altogether unexpected as the preparation of iron(II) complexes of mono/dipyridyl-pyrazolates, by Murray et al.[14] and Kaizaki et al.[15] were carried out under inert atmospheres.

To try to obtain the complex $[Fe^{II}_2(PMAP)_2](BF_4)_2$ a Schlenk line, ascorbic acid (*in situ* reductant) and strictly dry degassed solvents were used. The solvent volume was reduced, and the concentrated solution diffused with diethyl ether vapor resulting in the formation of a fine red powder. On one occasion, recrystallization, *in air*, from a concentrated ethanol/acetonitrile (5:1) solution layered with hexane gave large intensely dark red high quality single crystals suitable for X-ray diffraction. The structure determination confirmed it to be the *iron(III)* complex $[Fe^{III}_2(PMAP)_2](BF_4)_4 \cdot 2MeCN$ (vide infra). Isolation of these crystals, by filtration under nitrogen, directly followed by drying under vacuum, caused them to visibly deteriorate. Microanalytical data obtained on the resulting powder were very poor indicating that this Fe(III) complex is highly unstable. Attempts to remake it were successful only one other time (see Supporting Information for more experimental details and more detailed discussion).

Returning to our original goal, namely, the isolation of the unstable *iron(II)* complex, our attempts with BF_4^- as the counteranion failed (see Supporting Information for more details), so we decided to employ a different anion, SbF_6^- (chosen mainly because it was available in our laboratory, but also because such anions have been used to stabilize reactive cations/electrophiles[30]). Anhydrous $Fe^{II}(AcO)_2$ and PMAPH were reacted, in a 2:2 ratio at room temperature, in isopropanol-methanol 9:1 (this solvent mixture was used to induce faster precipitation thereby avoiding oxidation or degradation of the complex over time in solution), before addition of a methanolic solution of 2 equiv of $NaSbF_6$. The solution was filtered, and the filtrate placed in the freezer overnight. The resulting brown-yellow solid, $[Fe^{II}_2(PMAP)_2](SbF_6)_2 \cdot 2.25(C_3H_8O)$, was filtered off and dried under vacuum (56% yield). The microanalytical results are in agreement with the proposed formula, and the IR spectrum shows the characteristic bands of SbF_6^- at 667, 620, and 529 cm^{-1}. Attempts to improve the yield by adding potassium *tert*-butoxide to deprotonate the pyrazole ring resulted in the isolation of highly impure solids. The origin of this contamination is unclear.

X-ray Crystallography. Selected bond lengths and angles for the complexes $[M^{II}_2(PMAP)_2]X_2 \cdot 2MeCN$ where M = Zn or Cu and X = BF_4, or M = Ni and X = ClO_4, and $[Fe^{III}_2(PMAP)_2](BF_4)_4 \cdot 2MeCN$ (Figure 5 and Supporting Information, Figure S1) are presented in Table 1.

All of the crystals that were analyzed were grown by vapor diffusion of diethyl ether into acetonitrile solutions with the exception of the complex $[Fe^{III}_2(PMAP)_2](BF_4)_4 \cdot 2MeCN$ which was grown by layering hexane on an 1:5 acetonitrile/ethanol solution. The four structures are similar but the variability of the orientation of the arms and the willingness of the central metal ions to conform to an octahedral environment have created subtle differences between the structures.

In all the cases the molecule as a whole has a "sandwich" like configuration with the two metal centers encapsulated by the two ligands in an approximately octahedral geometry. Each terdentate binding pocket of the individual $PMAP^-$ ligands is coordinated to the metal ion in *facial* mode. Each individual ligand can also coordinate in a *cis*- or *trans*-axial mode around the metal centers (Figure 5 and

(28) Sigel, H.; Martin, R. B. *Chem. Rev.* **1982**, *82*, 385–426.
(29) Deacon, G. B.; Phillips, R. J. *Coord. Chem. Rev.* **1980**, *33*, 227–250.
(30) See for example: Krossing, I.; Raabe, I. *Chem.—Eur. J.* **2004**, *10*, 5017–5030. Krossing, I.; Raabe, I. *Angew. Chem., Int. Ed.* **2004**, *43*, 2066–2090.

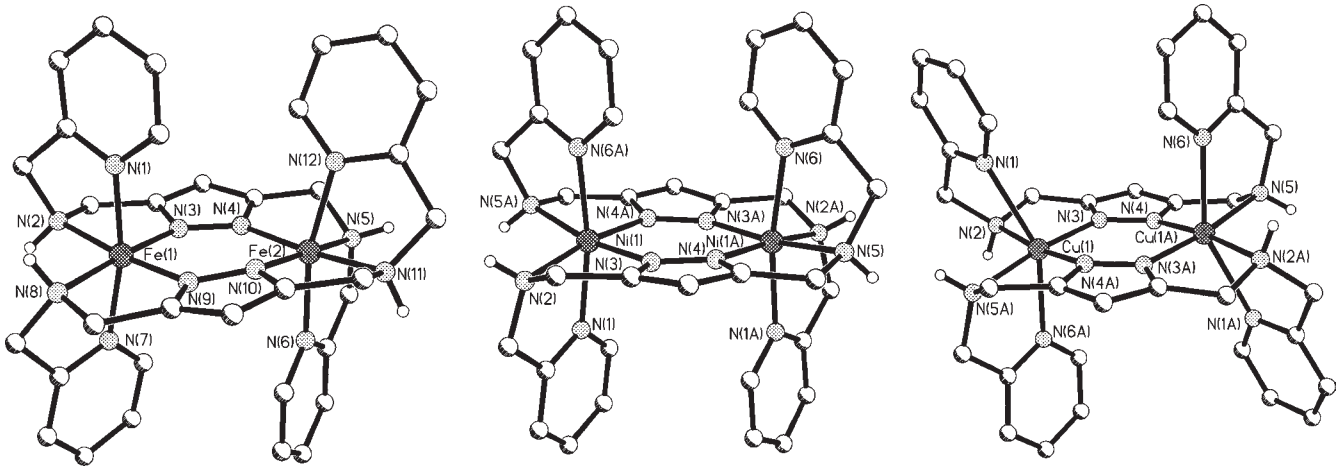

Figure 5. Molecular structure of the cations $[Fe^{III}_2(PMAP)_2]^{4+}$, $[Ni^{II}_2(PMAP)_2]^{2+}$, and $[Cu^{II}_2(PMAP)_2]^{2+}$, highlighting the *cis*- versus *trans*-ligand binding modes. $[Zn^{II}_2(PMAP)_2]^{2+}$ is isomorphous with $[Cu^{II}_2(PMAP)_2]^{2+}$. All hydrogen atoms, except those of the amine groups have been omitted for clarity.

Table 1. Tables of Bond Lengths and Angles for the Complexes $[Fe^{III}_2(PMAP)_2](BF_4)_4\cdot 2MeCN$, $[Ni^{II}_2(PMAP)_2](ClO_4)_2\cdot 2MeCN$, $[Cu^{II}_2(PMAP)_2](BF_4)_2\cdot 2MeCN$, and $[Zn^{II}_2(PMAP)_2](BF_4)_2\cdot 2MeCN$[a]

$[Fe^{III}_2(PMAP)_2](BF_4)_4\cdot 2MeCN$							
Fe(1)		Fe(2)			$[Zn^{II}_2(PMAP)_2]$-$(BF_4)_2\cdot 2MeCN$	$[Cu^{II}_2(PMAP)_2]$-$(BF_4)_2\cdot 2MeCN$	$[Ni^{II}_2(PMAP)_2]$-$(ClO_4)_2\cdot 2MeCN$
M−N(1)	1.9763(13)	M−N(4)	1.8953(12)	M−N(1)	2.1854(16)	2.4407(14)	2.0783(17)
M−N(2)	2.0336(13)	M−N(5)	2.0357(13)	M−N(2)	2.2898(17)	2.1095(14)	2.1660(19)
M−N(3)	1.8935(13)	M−N(6)	1.9675(13)	M−N(3)	2.0536(16)	1.9526(13)	2.0010(17)
M−N(7)	1.9706(13)	M−N(10)	1.8986(13)	M−N(4)	2.0492(16)	1.9485(13)	1.9998(17)
M−N(8)	2.0182(13)	M−N(11)	2.0182(13)	M−N(5)	2.3280(17)	2.1565(14)	2.1813(18)
M−N(9)	1.8935(13)	M−N(12)	1.9885(13)	M−N(6)	2.1379(16)	2.2785(14)	2.1034(17)
N(1)−M(1)−N(2)	82.34(5)	N(4)−M(1)−N(5)	79.59(5)	N(1)−M(1)−N(2)	74.91(6)	74.68(5)	80.31(7)
N(1)−M(1)−N(3)	95.38(5)	N(4)−M(1)−N(6)	95.59(5)	N(1)−M(1)−N(3)	102.399(6)	103.60(5)	94.70(7)
N(1)−M(1)−N(7)	168.71(5)	N(4)−M(1)−N(10)	94.67(5)	N(1)−M(1)−N(4)	99.53(6)	100.68(5)	93.68(7)
N(1)−M(1)−N(8)	91.69(5)	N(4)−M(1)−N(11)	172.79(5)	N(1)−M(1)−N(5)	84.84(6)	82.35(5)	94.18(7)
N(1)−M(1)−N(9)	92.96(5)	N(4)−M(1)−N(12)	94.29(5)	N(1)−M(1)−N(6)	151.93(6)	152.18(5)	169.93(7)
N(2)−M(1)−N(3)	82.15(5)	N(5)−M(1)−N(6)	84.42(5)	N(2)−M(1)−N(3)	76.82(6)	80.73(5)	78.78(7)
N(2)−M(1)−N(7)	89.43(5)	N(5)−M(1)−N(10)	172.99(5)	N(2)−M(1)−N(4)	170.52(6)	173.03(5)	171.85(7)
N(2)−M(1)−N(8)	100.21(5)	N(5)−M(1)−N(11)	103.89(5)	N(2)−M(1)−N(5)	109.74(6)	103.84(5)	106.44(7)
N(2)−M(1)−N(9)	174.61(5)	N(5)−M(1)−N(12)	88.18(5)	N(2)−M(1)−N(6)	91.50(6)	91.45(5)	93.77(7)
N(3)−M(1)−N(7)	95.38(5)	N(6)−M(1)−N(10)	92.19(5)	N(3)−M(1)−N(4)	97.24(6)	95.54(5)	96.36(7)
N(3)−M(1)−N(8)	176.52(5)	N(6)−M(1)−N(11)	91.07(5)	N(3)−M(1)−N(5)	171.49(6)	173.40(5)	170.37(7)
N(3)−M(1)−N(9)	95.38(5)	N(6)−M(1)−N(12)	166.39(5)	N(3)−M(1)−N(6)	98.07(6)	97.61(5)	92.10(7)
N(7)−M(1)−N(8)	82.13(5)	N(10)−M(1)−N(11)	82.27(5)	N(4)−M(1)−N(5)	76.94(6)	80.40(5)	79.33(7)
N(7)−M(1)−N(9)	95.58(5)	N(10)−M(1)−N(12)	96.32(5)	N(4)−M(1)−N(6)	96.70(6)	94.90(5)	92.94(7)
N(8)−M(1)−N(9)	82.49(5)	N(11)−M(1)−N(12)	79.62(5)	N(5)−M(1)−N(6)	76.70(6)	77.67(5)	79.60(7)
M···M (Å)	3.901				4.060	3.957	4.016
$\sum$[31]	63.8°		73.9°	$\sum$	124.9°	111.6°	86.2°

[a] $\sum$ = 110.5° for $[Mn^{II}_2(PMAP)_2](BPh_4)_2$.[8]

Scheme 1). This is easiest described as having the pendant pyridine arms both up (*cis*-axial; seen here for Cu^{II} and Zn^{II}; in both of these structures the two metal ions are related by a center of symmetry between them) or having a one up and one down (*trans*-axial; seen here for Fe^{III} and Ni^{II}; in the iron structure the two metal ions are crystallographically independent; for the nickel structure the two metal ions are related by a 2-fold axis between them).

An indication of the level of distortion of the complexes from O_h can be obtained by taking the sum of the deviation from 90° of the 12 *cis* angles ($\sum$) in the coordination sphere.[31] The greatest deviation from pure octahedral geometry of all of the complexes is exhibited by the zinc(II) (d^{10}) complex with a value of $\sum$ = 124.9°. This, however, is close to the values of 110.5° and 111.6° observed in the manganese(II) (d^5) complex of Okawa and co-workers[8] and the copper(II) (d^9) complex presented here. All three of these complexes exhibit the *cis*-axial coordination mode and as a result are clearly seen to display a higher degree of deviation from octahedral geometry with respect to $\sum$ and their bond angles. This preference for the *cis*-axial coordination mode is most

(31) Guionneau, P.; Brigouleix, C.; Barrans, Y.; Goeta, A. E.; Létard, J.-F.; Howard, J. A. K.; Gaultier, J.; Chasseau, D. *C. R. Acad. Sci. Paris, Chim.* **2001**, *4*, 161–171. Deeney, F. A.; Charles, J. H.; Morgan, G. G.; McKee, V.; Nelson, J.; Teat, S. J.; Clegg, W. *J. Chem. Soc., Dalton Trans.* **1998**, 1837–1843. Drew, M. G. B.; Harding, C. J.; McKee, V.; Morgan, G. G.; Nelson, J. *J. Chem. Soc., Chem. Commun.* **1995**, 1035–1038.

likely because all three of these metal ions can more readily deviate from pure O_h as they have no overriding preference for the O_h geometry. This is in contrast to the two other crystal structures, of iron(III) and nickel(II), which have values of $\sum$ between 63.8 and 86.2°. There is no crystallographic symmetry present within $[Fe^{III}_2(PMAP)_2](BF_4)_4 \cdot 2MeCN$ so unlike the three other complexes described here, it has two crystallographically independent metal centers with different values for $\sum$. These complexes have less deviation from the O_h coordination mode, probably because Fe^{III} is small and Ni^{II} has a preference for this coordination geometry. This is clearly seen in the pictures of the structures of each of these complexes as they have a more regular appearance. These complexes also exhibit the *trans* arrangement with respect to the ligand, which helps to give a more regular appearance when compared to the *cis*-axial coordination mode. The copper(II) complex also shows Jahn−Teller distortion of the axially coordinated pyridine moieties. This is clearly seen by comparison with the isomorphous zinc(II) complex (Cu−N_{ax} 2.44 and 2.28 Å; Zn−N_{ax} 2.19 and 2.14 Å).

Each of the complexes have two, doubly pyrazolate-bridged, metal centers. The Cu^{II}, Ni^{II}, and Zn^{II} complexes have metal-to-metal separations of 3.957, 4.016, and 4.060 Å, respectively. These separations lie within the ranges observed for similar pyrazole complexes, with 3,5-pendant coordinating arms, of copper(II)[4,32−34] (3.8147−4.066 Å), nickel(II)[34−36] (3.830−4.108 Å), and zinc(II)[33,37] (3.993−4.064 Å).

None of the complexes characterized appear to have any strong intramolecular $\pi-\pi$ interactions. Only the isostructural complexes of $[Cu^{II}_2(PMAP)_2](BF_4)_2 \cdot 2MeCN$ and $[Zn^{II}_2(PMAP)_2](BF_4)_2 \cdot 2MeCN$ appear to have strong intermolecular $\pi-\pi$ or T−π interactions present (Supporting Information, Figure S2). There is a parallel offset $\pi-\pi$ interaction of 3.45 Å between adjacent pyridine rings of two $[Cu^{II}_2(PMAP)_2]^{2+}$ cations. There are also two T−π interactions between the adjacent molecules: the stronger of the two is between the coordinated pyridine ring of one cation and the pyrazolate ring of the next cation. The pyridine ring of one molecule also sits directly above the five membered pyrazolate ring of the next. The second T−π interaction is again between adjacent pyridine rings of the two cations and is the weakest of the three interactions at 3.67 Å. It should be noted that it is possible that the *cis*- or *trans*-axial mode observed is also influenced by these packing interactions.

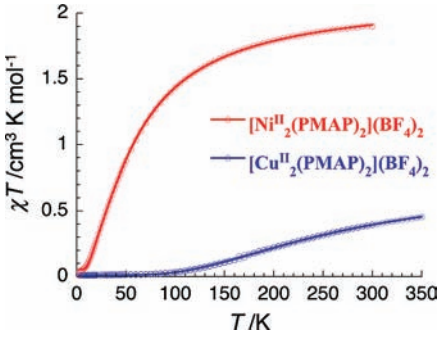

Figure 6. χT versus T plot (with χ being the magnetic susceptibility equal to M/H normalized per dinuclear complex) for $[Ni^{II}_2(PMAP)_2](BF_4)_2$ (red), $[Cu^{II}_2(PMAP)_2](BF_4)_2$ (blue) measured at 1000 Oe. The solid lines are the best fits obtained with the isotropic Heisenberg models described in the text.

Magnetic Studies. The magnetic properties of the $[Ni^{II}_2(PMAP)_2](BF_4)_2$ and $[Cu^{II}_2(PMAP)_2](BF_4)_2$ compound have been studied between 300 and 1.8 K. At room temperature, the χT products are 1.91 and 0.40 cm^3 K/mol respectively (Figure 6). These values are lower than expected for the presence of two $S = 1$ Ni^{II} ions ($S = 1$, $C = 1$ cm^3 K/mol with $g = 2$) and two $S = 1/2$ Cu^{II} ions ($S = 1/2$, $C = 0.375$ cm^3 K/mol with $g = 2$) suggesting the presence of intramolecular antiferromagnetic interaction between spin carriers. This hypothesis is confirmed by the temperature dependence of the χT product that decreases sweeping the temperature from 300 to 1.8 K and reaches about 0.01 cm^3 K/mol at 1.8 K. This extremely low χT value at 1.8 K indicates a singlet ground state for both compounds in agreement with intramolecular antiferromagnetic interactions (note that also shows the lack of a significant amount of paramagnetic impurities as often seen in compounds with a singlet ground state). To analyze the magnetic properties of these compounds, isotropic Heisenberg dimer models have been employed using the following definition of the spin Hamiltonian: $H = -2JS_MS_M$ with J being the intramolecular M···M magnetic interactions and S_M the spin of the metal ions: $S = 1$ and 1/2 for Ni(II) and Cu(II) metal ions. In the low field approximation, the expression of the susceptibility for both cases can be easily found in the literature, for example, in reference 38. Both models lead to an excellent data/theory agreement as shown Figure 6 with with $J/k_B = -24.7(2)$ K and $g = 2.10(2)$ for $[Ni^{II}_2(PMAP)_2](BF_4)_2$ and $J/k_B = -252(2)$ K and $g = 2.10(2)$ for $[Cu^{II}_2(PMAP)_2](BF_4)_2$.

The J value obtained for $[Cu^{II}_2(PMAP)_2](BF_4)_2$ is in agreement with the magnetic interactions found for reported similar acyclic pyrazole complexes with 3,5-pendant coordinating arms (J values in the range −215 to −310 K). Robert and co-workers found a quasi-linear structure-magnetism relationship between δ(CuNN) and the J value for a series of symmetrical and asymmetrical acyclic dipyrazolate complexes, where δ(CuNN) is the mean deviation from the optimum CuNN angle (130.8°) that gave the maximum J value (Figure 7).[39] In the case of $[Cu^{II}_2(PMAP)_2](BF_4)_2$, the δ(CuNN) parameter is small, that is, 0.58°, and the estimation of the magnetic interaction by the Robert's

(32) Lamarque, L.; Miranda, C.; Navarro, P.; Escarti, F.; Garcia-Espana, E.; Latorre, J.; Ramirez, J. A. *Chem. Commun.* **2000**, 1337–1338. Teichgraber, J.; Leibeling, G.; Dechert, S.; Meyer, F. *Z. Anorg. Allgem. Chem.* **2005**, *631*, 2613–2618. Mernari, B.; Abraham, F.; Lagrenee, M.; Drillon, M.; Legoll, P. *J. Chem. Soc., Dalton Trans.* **1993**, 1707–1711. Du, M.; Chen, S.-T.; Guo, Y.-M.; Bu, X. H.; Ribas, J. *J. Mol. Struct.* **2005**, *737*, 17–21.

(33) Miranda, C.; Escartí, F.; Lamarque, L.; Garcia-Espana, E.; Navarro, P.; Latorre, J.; Lloret, F.; Jimenez, H. R.; Yunta, M. J. R. *Eur. J. Inorg. Chem.* **2005**, 189–208.

(34) Kramer, R.; Fritsky, I. O.; Pritzkow, H.; Kovbasyuk, L. A. *J. Chem. Soc., Dalton Trans.* **2002**, 1307–1314.

(35) Röder, J. C.; Meyer, F.; Kaifer, E.; Pritzkow, H. *Eur. J. Inorg. Chem.* **2004**, 1646–1660.

(36) Casabo, J.; Pons, J.; Siddiqi, K. S.; Teixidor, F.; Molins, E.; Miravitlles, C. *J. Chem. Soc., Dalton Trans.* **1989**, 1401–1403.

(37) Zhang, J.-F.; Li, X.-H. *Acta Crystallogr., Sect. E* **2006**, *E62*, m125–m127.

(38) O'Connor, C. J. *Prog. Inorg. Chem.* **1982**, *29*, 203–283.

(39) Hanot, V. P.; Robert, T. D.; Kolnaar, J.; Haasnoot, J. G.; Reedijk, J.; Kooijman, H.; Spek, A. L. *Dalton Trans.* **1996**, 4275–4281.

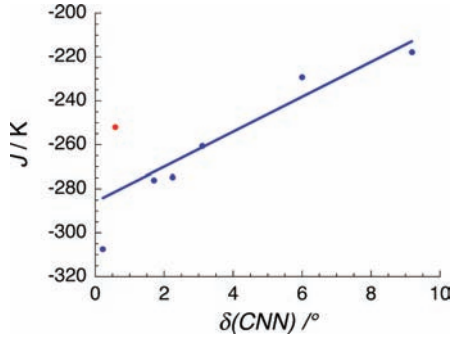

Figure 7. Variation of the magnetic interaction, J, versus δ(CNN) for nearly planar pyrazolato doubly bridged copper(II) complexes from reference 38. Obtained value for $[Cu^{II}_2(PMAP)_2](BF_4)_2$ is shown in red.

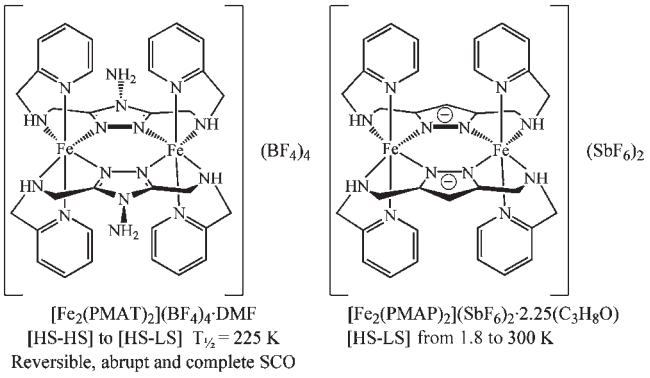

Figure 8. Expected structural similarities, and summary of the magnetic behavior, of the literature *triazole*-based complex $[Fe^{II}_2(PMAT)_2](BF_4)_4\cdot$DMF and the present *pyrazolate*-based complex $[Fe^{II}_2(PMAP)_2](SbF_6)_2\cdot 2.25(C_3H_8O)$.

correlation is not very accurate in this domain of δ(CuNN) (Figure 7). Nevertheless, the obtained J parameter falls in the range of expected values. In the case of $[Ni^{II}_2(PMAP)_2](BF_4)_2$, the obtained J value is in agreement with those reported for related dinuclear acyclic dipyrazolate complexes.[35,40]

As mentioned above, both X-ray crystallography and ^{57}Fe Mössbauer spectroscopy on the doubly-*triazole* bridged complex $[Fe^{II}_2(PMAT)_2](BF_4)_4\cdot$DMF showed that a SCO occurs, abruptly at 225 K, from [HS-HS] to [LS-HS] (not to a 50:50 mixture of [HS-HS]:[LS-LS]).[10] There was no evidence of a second SCO to the fully low spin [LS-LS] form even under pressure.[17] These intriguing results and the anticipated structural similarities between triazole-based $[Fe^{II}_2(PMAT)_2]^{4+}$ and pyrazolate-based $[Fe^{II}_2(PMAP)_2]^{2+}$ (Figure 8) were the key reasons the $[Fe^{II}_2(PMAP)_2]^{2+}$ complex was prepared. Clearly the magnetic behavior of this complex was expected to be far more interesting than that of the Cu(II) and Ni(II) analogues.

To avoid any solvent loss or sample degradation, the measurements (Figure 9) were started at 270 K, at 1000 Oe, and collected decreasing the temperature to 1.8 K. The field was then increased to 10000 Oe and data collected from 1.8 K up to 350 K before decreasing the temperature to 250 K. At room temperature (before

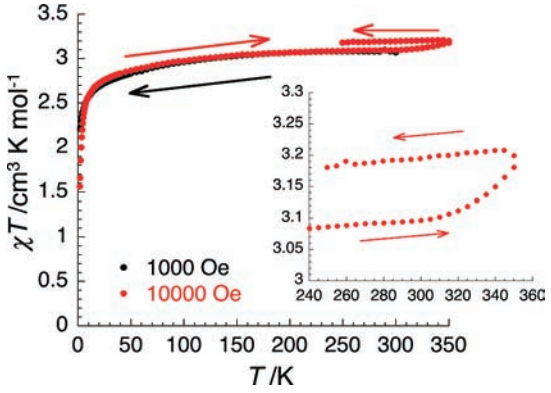

Figure 9. χT versus T plot for $[Fe^{II}_2(PMAP)_2](SbF_6)_2\cdot 2.25(C_3H_8O)$. Black dots shows cooling from room temperature to 1.8 K (at 1000 Oe). Red dots shows subsequent warming from 1.8 to 350 K, then on cooling back to 250 K (at 10000 Oe).

exposure to temperatures higher than 300 K), the χT product is equal to 3.1 cm^3 K mol^{-1}, corresponding to the expected value of 3 cm^3 K mol^{-1} for the presence of one $S = 2$ iron(II) and one LS state ($S = 0$) iron(II) metal ion, that is, a sample where 50% of the iron centers are in the HS and the other 50% are in the LS state. When the temperature is lowered, the χT product at 1000 Oe decreases, reaching a value of 2.2 cm^3 K mol^{-1} at 1.8 K indicating only weak intramolecular antiferromagnetic interactions and/or most likely spin−orbit coupling/anisotropy from the HS iron(II) metal ion. As for $[Fe^{II}_2(PMAT)_2](BF_4)_2\cdot$DMF, there is no sign of a fully LS form, [LS-LS], even at 1.8 K.

When the compound is warmed from 300 to 350 K the χT product increases slightly (Figure 9). This behavior could be due to a number of factors, for example, indicating (i) sample oxidation and/or (ii) degradation or (iii) that some of the [HS-LS] state sample converts to the fully HS, [HS-HS], species with associated isopropanol solvent loss. The last hypothesis is not uncommon in the literature. A particularly relevant example is the solvent-dependent SCO behavior seen in the system $[Fe^{II}(3\text{-bpp})_2]X_2\cdot$solvent (where 3-bpp = 2,6-bis(3-pyrazolyl)-pyridine and X = monoanion) in which the uncoordinated NH of the external pyrazole moieties hydrogen bond to solvent molecules or anions.[41] Hydrogen bond interactions may well be present in $[Fe^{II}_2(PMAP)_2](SbF_6)_2\cdot 2.25(C_3H_8O)$ also, but in this case the donor would be the coordinated secondary aliphatic amines of the pendant arms of the PMAP$^-$ ligand. As expected the [LS-HS] to [HS-HS] SCO temperature for $[Fe^{II}_2(PMAP)_2](SbF_6)_2\cdot 2.25(C_3H_8O)$, if indeed it is SCO active, is higher than that observed for the triazole-based analogue $[Fe^{II}_2(PMAT)_2](BF_4)_4\cdot$DMF (225 K), because of the negatively charged pyrazolate ligand conferring a stronger field on iron(II). Although there is no crystal structure for $[Fe^{II}_2(PMAP)_2](SbF_6)_2\cdot 2.25(C_3H_8O)$, it is highly likely that the "[HS-LS]" state is the same [HS-LS] state as seen for $[Fe^{II}_2(PMAT)_2](BF_4)_4\cdot$DMF, rather than a 1:1 mixture of [LS-LS]:[HS-HS], because of the

(40) Ball, P. W.; Blake, A. B. *J. Chem. Soc. A* **1969**, 1415–1422. Ishikawa, R.; Fuyuhiro, A.; Hayami, S.; Inoue, K.; Kawata, S. *J. Mol. Struct.* **2008**, *892*, 220–224.

(41) Sugiyarto, K. H.; Goodwin, H. A. *Aust. J. Chem.* **1988**, *41*, 1645–1663. Buchen, T.; Gütlich, P.; Goodwin, H. A. *Inorg. Chem.* **1994**, *33*, 4573–4576. Sugiyarto, K. H.; Craig, D. C.; Rae, A. D.; Goodwin, H. A. *Aust. J. Chem.* **1994**, *47*, 869–890.

strong structural similarities between the PMAPH and PMAT systems (Figure 8).

Conclusions

We have synthesized the pyrazole containing ligand, PMAPH, by a different route to the one previously published by Okawa and co-workers. This bis-terdentate ligand was reacted with a range of transition metal salts (Fe(II), Fe(III), Ni(II), Cu(II), Zn(II) metal ions), giving doubly pyrazolate-bridged dinuclear complexes of the form $[M^{II/III}_2(PMAP)_2](X)_{2/4}$. Four of the complexes have been structurally characterized. The choice of the metal ion was shown to control the coordination mode of the ligand. The *trans*-axial coordination mode of $PMAP^-$ was observed for the two nickel(II) and iron(III) metal centers, while the *cis*-axial coordination mode was observed for copper(II) and zinc(II), presumably facilitated by the latter metal ions being able to more readily adopt a distorted octahedral geometry.

The analogous iron(II) complex was found to be air sensitive and could only be obtained by using a bulky anion, SbF_6^-. $[Fe^{II}_2(PMAP)_2](SbF_6)_2 \cdot 2.25(C_3H_8O)$ was determined to be in a [HS-LS] state from 300 K down to 1.8 K. An X-ray crystal structure determination would be necessary to identify the exact nature of the [HS-LS] state complex; however, crystals of this air sensitive complex have not been forthcoming.

Experimental Section

Reagent grade methanol and ethanol were refluxed and distilled over magnesium turnings and iodine prior to use. HPLC grade acetonitrile was refluxed over calcium hydride before use. The 3,5-(1*H*)-pyrazoledicarbaldehyde was prepared as described in the literature.[27] The ^{1}H and ^{13}C NMR were recorded on a Varian INOVA-300 (or INOVA-500) spectrophotometer at 25 °C. Elemental analyses were carried out by the Campbell Microanalytical Laboratory at the University of Otago. IR spectra were recorded over the range 4000−400 cm^{-1} with a Perkin-Elmer Spectrum NBX FT-IR spectrophotometer as potassium bromide pellets. Electrospray Ionization (ESI) mass spectra were recorded using a Bruker MicrOTOF$_Q$ spectrometer. X-ray data (Table 2) were collected with a Bruker Kappa Apex II area detector using graphite-monochromated Mo−K_α radiation (λ = 0.71073 Å). The structures of all the complexes were solved using SHELXS-97.[42] All structures were refined against F^2 using all data by full matrix least-squares techniques with SHELXL-97.[42] All H-atoms were inserted in calculated positions and rode on the attached non-H atom, except for the NH protons, which were located from difference maps and freely refined. All other hydrogen atoms were given isotropic displacement parameters 1.2 times that of the attached non-H atom. Crystallographic data have been deposited with the Cambridge Crystallographic Data Centre (reference numbers CCDC 668742, 668743, 668744, and 668745 for $[Fe^{III}_2(PMAP)_2](BF_4)_4 \cdot 2MeCN$, $[Ni^{II}_2(PMAP)_2](ClO_4)_2 \cdot 2MeCN$, $[Cu^{II}_2(PMAP)_2](BF_4)_2 \cdot 2MeCN$, and $[Zn^{II}_2(PMAP)_2](BF_4)_2 \cdot 2MeCN$). The magnetic susceptibility measurements were obtained with the use of a Quantum Design SQUID magnetometer MPMS-XL housed at the Centre de Recherche Paul Pascal. This magnetometer operates between 1.8 and 300 K for direct current (dc) applied fields ranging from −7 to 7 T. Measurements were performed on polycrystalline samples of 10.89, 24.25, and 23.98 mg for $[Fe^{II}_2(PMAP)_2](SbF_6)_2 \cdot 2.25(C_3H_8O)$, $[Ni^{II}_2(PMAP)_2](BF_4)_2$, and $[Cu^{II}_2(PMAP)_2](BF_4)_2$. The magnetic data were corrected for the sample holder and the diamagnetic contributions. Before any measurement, the samples have been checked for the presence of ferromagnetic impurities by measuring the magnetization as a function of the field at 100 K. For pure paramagnetic or diamagnetic systems, a perfect straight line is expected and is observed for these compounds indicating the absence of any ferromagnetic impurities.

Caution! *While no problems were encountered during the course of this work, perchlorate salts are potentially* ***explosive*** *and should be handled with appropriate care at all times.*

Synthesis of PMAPH Ligand. To a pale yellow solution of 3,5-(1*H*)-pyrazoledicarbaldehyde (0.50 g, 4.0 mmol) in methanol (15 mL) was added a pale yellow solution of 2-(aminomethyl)pyridine (0.87 g, 8.0 mmol) in methanol (5 mL). After 30 min an excess of powdered sodium borohydride (1.51 g, 40.0 mmol) was added portion wise to the solution carefully by spatula over 15 min. The solution effervesced upon addition of the sodium borohydride. After an hour, water (10 mL) was added to the solution, which turned opaque and then cleared. The aqueous methanolic solution was extracted with chloroform (3 × 30 mL). The organic layer was washed once with distilled water and then dried over sodium sulfate, and the solvent removed under reduced pressure to leave the product (1.04 g, 85%) as a light yellow viscous oil. The material was promptly used in subsequent reactions (as an acetonitrile stock solution) without any further purification. ^{1}H NMR (500 MHz, $CDCl_3$): δ = 3.79 (d, 4H, 2 × PyC$\underline{H}_2$NH), 3.92 (d, 4H, 2 × NHC$\underline{H}_2$Pz), 6.09 (s, 1H, PzH), 7.11 (d, 2$\underline{H}$, 5-PyH), 7.25 (t, 2H, 3-Py$\underline{H}$), 7.57 (t, 2H, 4-PyH), 8.50 (d, 2H, 6-PyH). ^{13}C(^{1}H) NMR (125 MHz, $CDCl_3$): δ = 44.9 (2 × Pz$\underline{C}H_2$), 53.7 (2 × Py$\underline{C}H_2$), 97.5 (1 × Pz$\underline{C}$), 122.4 (2 × 5-Py$\underline{C}$), 122.9 (2 × 3-Py$\underline{C}$), 136.8 (2 × 4-Py$\underline{C}$), 145.8 (2 × Pz$\underline{C}$), 149.3 (2 × 6-Py$\underline{C}$), 158.0 (2 × 2-Py$\underline{C}$). ESI: found $PMAPH_2^+$ 309.1844, $C_{17}H_{21}N_6$ requires 309.1822.

$[Ni^{II}_2(PMAP)_2](ClO_4)_2 \cdot MeCN$. A pale blue solution of $Ni(ClO_4)_2 \cdot 6H_2O$ (0.296 g, 0.809 mmol) in acetonitrile (3 mL) was added dropwise to a colorless solution of PMAPH (0.250 g, 0.809 mmol) in acetonitrile (10 mL). The resulting pink solution was stirred overnight. A pink solid (0.115 g, 29% yield) precipitated which was collected and washed with acetonitrile and diethyl ether. Elemental analysis calcd. for $[Ni^{II}_2(PMAP)_2](ClO_4)_2 \cdot MeCN$ (M_r = 972.09 g mol^{-1}): C 44.48, H 4.25, N 18.73, Cl 7.29; found: C 44.50, H 4.37, N 19.07, Cl 7.34. IR (KBr): 3421, 3318, 3201, 3061, 2919, 1605, 1573, 1487, 1469, 1442, 1310, 1086, 1051, 901, 759, 626, 420 cm^{-1}. ESI: found $[Ni^{II}_2(PMAP)_2]^{2+}$ 365.1161, $C_{34}H_{38}N_{12}Ni_2$ requires 730.2038 (365.1019). Vapor diffusion of diethyl ether into the reaction filtrate gave pink single crystals of $[Ni^{II}_2(PMAP)_2](ClO_4)_2 \cdot 2MeCN$ (additional 0.085 g, 21% yield).

$[Ni^{II}_2(PMAP)_2](BF_4)_2 \cdot 1.5H_2O$. A pale blue solution of $Ni(BF_4)_2 \cdot 6H_2O$ (0.210 g, 0.620 mmol) in acetonitrile (5 mL) was added dropwise to a colorless solution of PMAPH (0.190 g, 0.620 mmol) in acetonitrile (10 mL). To the resulting pink solution was added triethylamine (0.062 g, 0.620 mmol). The pink solution was stirred overnight. Vapor diffusion of diethyl ether into the reaction filtrate gave pink crystals of $[Ni^{II}_2(PMAP)_2](BF_4)_2 \cdot 3H_2O$. A second recrystallization from acetonitrile by diethyl ether vapor diffusion gave pink crystals of $[Ni^{II}_2(PMAP)_2](BF_4)_2 \cdot 1.5H_2O$ (0.110 g, 38% yield). Elemental analysis calcd. for $[Ni^{II}_2(PMAP)_2](BF_4)_2 \cdot 1.5H_2O$ (M_r = 932.76 g mol^{-1}): C 43.70, H 4.44, N 17.98; found: C 43.64, H 4.58, N 17.89. IR (KBr): 3427, 3342, 3198, 2922, 1605, 1574, 1488, 1443, 1083, 1051, 901, 760, 522 cm^{-1}. ESI: found $[Ni^{II}_2(PMAP)_2]BF_4^+$ 817.2069 $C_{34}H_{38}N_{12}Ni_2BF_4$ requires 817.2079.

$[Cu^{II}_2(PMAP)_2](BF_4)_2 \cdot H_2O$. A blue solution of $Cu(BF_4)_2 \cdot 6H_2O$ (0.101 g, 0.292 mmol) in acetonitrile (3 mL) was added dropwise to a colorless solution of PMAPH (0.090 g, 0.292 mmol) in acetonitrile (5 mL). To the resulting deep blue solution was added triethylamine (0.029 g, 0.292 mmol). The resulting aquamarine colored solution was stirred overnight and a light

(42) Sheldrick, G. M. *Acta Crystallogr., Sect. A* **2008**, *A64*, 112–122.

Table 2. Crystallographic Data for the Complexes $[Fe^{III}_2(PMAP)_2](BF_4)_4\cdot 2MeCN$, $[Ni^{II}_2(PMAP)_2](ClO_4)_2\cdot 2MeCN$, $[Cu^{II}_2(PMAP)_2](BF_4)_2\cdot 2MeCN$, and $[Zn^{II}_2(PMAP)_2](BF_4)_2\cdot 2MeCN$

	$[Fe^{III}_2(PMAP)_2]$-$(BF_4)_4\cdot 2MeCN$	$[Ni^{II}_2(PMAP)_2]$-$(ClO_4)_2\cdot 2MeCN$	$[Cu^{II}_2(PMAP)_2]$-$(BF_4)_2\cdot 2MeCN$	$[Zn^{II}_2(PMAP)_2]$-$(BF_4)_2\cdot 2MeCN$
empirical formula	$C_{38}H_{44}B_4F_{16}N_{14}Fe_2$	$C_{38}H_{44}Cl_2N_{14}O_8Ni_2$	$C_{38}H_{44}B_2F_8N_{14}Cu_2$	$C_{38}H_{44}B_2F_8N_{14}Zn_2$
formula weight (g mol^{-1})	1155.81	1013.19	997.57	1001.23
crystal system	triclinic	monoclinic	triclinic	triclinic
space group	$P\bar{1}$	$C2/c$	$P\bar{1}$	$P\bar{1}$
a (Å)	10.8017(11)	26.478(3)	9.5036(3)	9.4553(3)
b (Å)	12.3406(9)	15.4941(16)	10.5615(3)	10.6452(4)
c (Å)	19.6573(11)	11.1864(12)	11.8661(4)	11.8977(4)
α (deg)	84.539(2)	90	86.165(2)	85.717(2)
β (deg)	77.484(2)	110.728(4)	79.472(2)	80.072(2)
γ (deg)	65.603(3)	90	64.1210(10)	64.1380(10)
V (Å^3)	2329.6(3)	4292.1(8)	1053.44(6)	1061.47(6)
Z	2	4	1	1
$\rho_{calcd.}$ (g cm^{-3})	1.648	1.568	1.572	1.566
μ (mm^{-1})	0.736	1.071	1.094	1.214
temperature (K)	89(2)	89(2)	89(2)	89(2)
F(000)	1172	2096	510	512
crystal color and shape	deep red block	pink block	blue block	colorless cube
crystal size (mm^3)	0.45 × 0.3 × 0.2	0.18 × 0.14 × 0.10	0.24 × 0.20 × 0.12	0.20 × 0.20 × 0.20
$\Theta_{min.}/\Theta_{max.}$ (deg)	2.21/26.46	2.80/26.45	2.14/26.45	2.44/26.38
h	−13 → 13	−33 → 33	−11 → 11	−11 → 11
k	−15 → 15	−14 → 14	−13 → 13	−13 → 13
l	−24 → 24	−19 → 19	−14 → 14	−14 → 14
reflection collected/R(int)	45838/0.0310	4395/0.0322	22882/0.0254	22624/0.0294
data/restraints/parameter	9582/28/746	4395/0/334	4305/0/298	4340/0/298
GOF	1.041	1.037	1.088	1.048
$R1/wR2$ [$I > 2\sigma(I)$]	0.0281/0.0750	0.0322/0.0823	0.0251/0.0688	0.0294/0.0768
$R1/wR2$ (all data)	0.0380/0.0770	0.0409/0.0886	0.0271/0.0703	0.0323/0.0792
max. peak/hole (e Å^{-3})	0.518/−0.405	0.423/−0.340	0.424/−0.343	0.497/−0.357

blue solid precipitated out of solution which was collected and washed with acetonitrile and diethyl ether (0.085 g, 63% yield). Elemental analysis calcd. for $[Cu^{II}_2(PMAP)_2](BF_4)_2\cdot H_2O$ (M_r = 933.47 g mol^{-1}): C 43.75, H 4.32, N 18.01; found: C 43.78, H 4.20, N 18.11. IR (KBr): 3452, 3330, 2931, 1594, 1476, 1436, 1304, 1247, 1084, 907, 892, 761, 624, 533, 521 cm^{-1}. ESI: found $[Cu^{II}_2(PMAP)_2]^+$ (-H$^+$) 739.1914, $C_{34}H_{37}N_{12}Cu_2$ requires 739.1851. Vapor diffusion of diethyl ether into an acetonitrile solution of the complex gave large blue clusters of crystals of $[Cu^{II}_2(PMAP)_2](BF_4)_2\cdot 2MeCN$.

$[Cu^{II}_2(PMAP)_2](ClO_4)_2\cdot 3MeCN$. A blue solution of $Cu(ClO_4)_2\cdot 6H_2O$ (0.300 g, 0.809 mmol) in acetonitrile (3 mL) was added dropwise to a clear solution of PMAPH (0.250 g, 0.809 mmol) in acetonitrile (10 mL). To the resulting deep blue solution was added triethylamine (0.082 g, 0.809 mmol), giving an aquamarine colored solution that was stirred overnight. The resulting precipitate was collected and washed with acetonitrile and diethyl ether (0.233 g, 54% yield). Elemental analysis calcd. for $[Cu_2(PMAP)_2](ClO_4)_2\cdot 3MeCN$ (M_r = 1063.91 g mol^{-1}): C 45.16, H 4.45, N 19.75; found: C 45.18, H 4.60, N 19.76; IR (KBr): 3450, 3384, 3273, 3196, 2931, 2868, 1594, 1570, 1508, 1476, 1436, 1370, 1316, 1247, 1087, 996, 892, 761, 624 cm^{-1}. ESI: found $[Cu^{II}_2(PMAP)_2]^+$ (-H$^+$) 739.1874, $C_{34}H_{37}N_{12}Cu_2$ requires 739.1851.

$[Cu^{II}_2(PMAP)_2](NO_3)_2\cdot 2.5H_2O$. A blue solution of $Cu(NO_3)_2\cdot 3H_2O$ (0.071 g, 0.292 mmol) in acetonitrile (3 mL) was added dropwise to a clear solution of PMAPH (0.090 g, 0.292 mmol) in acetonitrile (5 mL). A light blue precipitate formed to which triethylamine (0.029 g, 0.292 mmol) was added. This resulted in a green solution which was stirred overnight. Vapor diffusion of diethyl ether into the reaction solvent gave light blue solid which was collected and washed with diethyl ether (0.046 g, 35% yield). Elemental analysis calcd. for $[Cu_2(PMAP)_2](NO_3)_2\cdot 2.5H_2O$ (M_r = 904.98 g mol^{-1}): C 45.28, H 4.69, N 21.74; found: C 45.48, H 4.72, N 21.76; IR (KBr): 3446, 3253, 2939, 1594, 1476, 1383, 1354, 1248, 1217, 1043, 1003, 907, 893, 830, 764, 624 cm^{-1}. ESI: found $[Cu^{II}_2(PMAP)_2]^+$ (-H$^+$) 739.1973, $C_{34}H_{37}N_{12}Cu_2$ requires 739.1851.

$[Cu^{II}_2(PMAP)_2](OAc)_2\cdot 2.5H_2O$. A blue solution of $Cu(OAc)_2\cdot H_2O$ (0.071 g, 0.292 mmol) in acetonitrile (3 mL) was added dropwise to a clear solution of PMAPH (0.090 g, 0.292 mmol) in acetonitrile (5 mL). This resulted in a blue solution which was stirred overnight. Vapor diffusion of diethyl ether into the reaction solution gave a blue solid which was collected and washed with diethyl ether (0.042 g, 32% yield). Elemental analysis calcd. for $[Cu_2(PMAP)_2](OAc)_2\cdot 2.5H_2O$ (M_r = 904.98 g mol^{-1}): C 50.43, H 5.46, N 18.57; found: C 50.44, H 5.43, N 18.76; IR (KBr): 3381, 1568, 1475, 1404, 1302, 1246, 1150, 1089, 1042, 997, 912, 892, 819, 761, 624 cm^{-1}. ESI: found $[Cu^{II}_2(PMAP)_2]^+$ (-H$^+$) 739.1893, $C_{34}H_{37}N_{12}Cu_2$ requires 739.1851.

$[Zn^{II}_2(PMAP)_2](BF_4)_2\cdot H_2O$. A colorless solution of PMAPH (0.090 g, 0.292 mmol) in acetonitrile (3 mL) was added dropwise to solid potassium *tert*-butoxide (0.033 g, 0.292 mmol) which dissolved slowly over 30 min giving a very pale yellow solution. To the resulting pale yellow solution was added a colorlesss solution of $Zn(BF_4)_2\cdot 6H_2O$ (0.101 g, 0.292 mmol) in acetonitrile (5 mL). The resulting coloress solution was stirred overnight. Vapor diffusion of diethyl ether into the reaction solution gave large colorless clusters of crystals which were collected and washed with diethyl ether (0.070 g, 52% yield). Elemental analysis calcd. for $[Zn^{II}_2(PMAP)_2](BF_4)_2\cdot H_2O$ (M_r = 937.14 g mol^{-1}): C 43.58, H 4.30, N 17.94; found: C 43.78, H 4.21, N 17.99; IR (KBr): 3451, 3391, 3260, 3214, 2912, 1602, 1572, 1482, 1438, 1301, 1268, 1249, 1052, 1034, 904, 888, 764, 641, 627 cm^{-1}. ^{1}H NMR (500 MHz, CD_3CN): δ = 3.58, 4.33 (4H, 2 × PzC$\underline{H}_2$NH), 3.87, 4.41 (4H, 2 × NHC$\underline{H}_2$Py), 5.81 (1H, PzH), 7.28 (2H, 5-PyH), 7.33 (2H, 3-PyH), 7.87 (2H, 4-PyH), 7.97 (2H, 6-PyH). ^{13}C(^{1}H) NMR (125 MHz, CD_3CN): δ = 48.3 (2 × PzCH$_2$), 53.9 (2 × PyCH$_2$), 96.6 (1 × PzC), 124.7 (2 × 5-PyC), 124.8 (2 × 3-PyC), 140.4 (2 × 4-PyC), 147.6 (2 × 6-PyC), 151.3 (2 × PzC), 157.6 (2 × 2-PyC). ESI: found $[Zn^{II}_2(PMAP)_2]^+$ (-H$^+$) 371.1056, $C_{34}H_{37}N_{12}Zn_2$ requires 371.0957.

$[Fe^{III}_2(PMAP)_2](BF_4)_4\cdot 2MeCN$. Under nitrogen a colorless solution of PMAPH (0.075 g, 0.223 mmol) in acetonitrile was added to solid potassium *tert*-butoxide (0.027 g, 0.223 mmol).

A suspension formed initially, and then, slowly over 30 min, the base dissolved to give a slightly yellow color. To this was added a colorless solution of $Fe^{II}(BF_4)_2 \cdot 6H_2O$ (0.082 g, 0.223 mmol) in acetonitrile (5 mL) which resulted in a dark orange solution which was stirred for 2 h. The solution was subjected to diethyl ether vapor diffusion under a nitrogen atmosphere giving a deep red precipitate. High quality single crystals of this powder were grown by dissolving the material in a minimum of acetonitrile (1 mL) and then adding EtOH (5 mL). This solution was then layered with hexane and left to sit for 10 days whereupon large regular diamond-like single crystals of $[Fe^{III}{}_2(PMAP)_2](BF_4)_4 \cdot 2MeCN$ formed. Once exposed to air the crystals degraded.

$[Fe^{II}{}_2(PMAP)_2](SbF_6)_2 \cdot 2.25(C_3H_8O)$. Under nitrogen a degassed solution of $Fe^{II}(OAc)_2$ (0.068 g, 0.39 mmol) in 5 mL of methanol were added to a degassed colorless solution of PMAPH (0.119 g, 0.39 mmol) in isopropanol-methanol (9:1) mixture. The resulting red solution was stirred for 2 h under nitrogen, then 5 mL of a colorless methanolic solution of $NaSbF_6$ (0.100 g, 0.39 mmol) were added, and the solution was stirred for 1 h. The resulting dark red solution was filtered, and the filtrate placed in the freezer overnight. The next day a brown-yellow solid was filtered and dried under vacuum resulting in a brown yellow powder (50.8 mg, 56% yield). Elemental analysis calcd for $[Fe^{II}{}_2(PMAP)_2](SbF_6)_2 \cdot 2.25(C_3H_8O)$ (M_r = 1333.15 g mol^{-1}): C 36.71, H 4.23, N 12.61; found: C 37.17, H 3.75, N 13.11; IR (KBr): 3413, 2961, 2920, 2820, 1653, 1607, 1539, 1478, 1441, 1041, 768, 667, 620 449 cm^{-1}. ESI: found $[Fe_2(PMAP)_2]^{2+}$ 363.0977 requires 363.1016.

Acknowledgment. This research was supported by grants from the University of Otago, the MacDiarmid Institute for Advanced Materials and Nanotechnology, the Marsden Fund (RSNZ), the University of Bordeaux, the CNRS, the European Network of Excellence: MAGMANet (NMP3-CT-2005-515767), the GIS Advanced Materials in Aquitaine (COMET Project) and the Région Aquitaine.

Supporting Information Available: Includes a molecular structure diagram of the $[Zn^{II}{}_2(PMAP)_2]^{2+}$ cation and of the intermolecular interactions present in $[Cu^{II}{}_2(PMAP)_2](BF_4)_2 \cdot 2MeCN$. Further experimental details and discussion of the Fe(III) and Fe(II) coordination chemistry are also included. This material is available free of charge via the Internet at http://pubs.acs.org.